# Radiation Induced Checkpoint Immunotherapy Response in Refractory Colorectal and Pancreatic Adenocarcinoma

**Aparna Parikh**
Massachusetts General Hospital https://orcid.org/0000-0002-5245-7841
**Annamaria Szabolcs**
Massachusetts General Hospital
**Jill Allen**
Massachusetts General Hospital
**Jeffrey Clark**
Massachusetts General Hospital
**Jennifer Wo**
Massachusetts General Hospital
**Hannah Thel**
Massachusetts General Hospital
**David Hoyos**
Memorial Sloan Kettering Cancer Center
**Arnav Mehta**
Massachusetts General Hospital
**Sanya Arshad**
Massachusetts General Hospital
**David Lieb**
Broad Institute
**Lorraine Drapek**
Massachusetts General Hospital
**Lawrence Blaszkowsky**
Massachusetts General Hospital
**Bruce Giantonio**
Massachusetts General Hospital
**Colin Weekes**
Massachusetts General Hospital
**Andrew Zhu**
Massachusetts General Hospital
**Lipika Goyal**

Massachusetts General Hospital
**Ryan Nipp**
Massachusetts General Hospital
**Jon Dubois**
Massachusetts General Hospital
**Emily van Seventer**
Massachusetts General Hospital
**Bronwen Foreman**
Massachusetts General Hospital
**Lauren Matlack**
Massachusetts General Hospital
**Leilana Ly**
Massachusetts General Hospital
**Jessica Meurer**
Massachusetts General Hospital
**Nir Hacohen**
Broad Institute https://orcid.org/0000-0002-2349-2656
**David Ryan**
Massachesetts General Hospital
**Beow Yeap**
Massachusetts General Hospital
**Ryan Corcoran**
Massachusetts General Hospital
**Benjamin Greenbaum**
Memorial Sloan Kettering Cancer Center
**David Ting** ( DTING1@mgh.harvard.edu )
Massachusetts General Hospital https://orcid.org/0000-0002-3261-2322
**Theodore Hong**
Massachusetts General Hospital

---

**Article**

**Keywords:** Radiation, Induced Checkpoint Immunotherapy, Refractory Colorectal, Pancreatic Adenocarcinoma

**Posted Date:** September 1st, 2020

**DOI:** https://doi.org/10.21203/rs.3.rs-58489/v1

**Version of Record:** A version of this preprint was published at Nature Cancer on November 18th, 2021.
See the published version at https://doi.org/10.1038/s43018-021-00269-7.

# Abstract

Immune checkpoint blockade has limited efficacy in microsatellite stable (MSS) colorectal (CRC) and pancreatic (PDAC) cancer. Preclinical models have demonstrated the use of radiation to activate the innate immune response and stimulate responsiveness to immune checkpoint blockade. Here, we describe a Phase 2 trial of radiation therapy combined with combined anti-CTLA4 (ipilimumab) and anti-PD1 (nivolumab) antibodies in MSS CRC and PDAC. In the per protocol analysis disease control rate was 37% (10/27) in CRC and 29% (5/17) in PDAC with an overall response rate of 15% (4/27) and 18% (3/17), respectively. Whole exome and RNA sequencing of biopsies from 17 patients revealed low tumor mutational burden in all tumors, but a notable upregulation of interferon stimulated genes with concordant high expression of multiple repeat RNA transcripts in responders. Altogether, this study provides foundational human proof of concept of radiation with combination immune checkpoint blockade therapy in otherwise immunotherapy resistant cancers.


# Introduction

Metastatic colorectal cancer (CRC) and pancreatic ductal adenocarcinoma (PDAC) remains incurable for the vast majority of patients. While significant advances have been made with cytotoxic chemotherapy combinations and to lesser extent biologics in CRC, virtually all patients with unresectable disease will die from the cancer within 5 years[1]. Similarly, while cytotoxic chemotherapy such as FOLFIRINOX has improved short term outcomes in PDAC, longer term outcomes remain dismal[2]. Immunotherapy represents a promising development in the treatment of cancer, but has had limited efficacy in microsatellite stable (MSS) CRC and PDAC[3]. Both single-agent and dual-agent immunotherapy has been tried with limited efficacy[4–6]. Most recently, a study of an anti-PD-L1 monoclonal antibody (durvalumab) given as monotherapy or in combination with an anti-CTLA4 monoclonal antibody (tremelimumab) in patients with metastatic PDAC was ineffective with response rates of 0% and 3% respectively[5]. The only group that reliably responds to immunotherapy are patients with tumors that have microsatellite instability, presumably due to the high mutational rate leading to a large neoantigen burden. In a seminal study by Le and colleagues, patients with mismatch-repair deficient colorectal cancers had a 40% response rate to pembrolizumab. In contrast, no patients with a MSS colorectal cancer responded[3,7]. Similarly Keynote-158 showed some PDAC responses, but only in the rare subset of MSI positive patients[8,9].

Radiation therapy has been suggested as a modality that may increase the likelihood of systemic response to immunotherapy via a phenomenon known as the abscopal effect in which local treatment of a tumor leads to antitumor response at distant sites[10,11,12]. Most recently, data in non-small cell lung cancer demonstrated that treatment with anti-PD1 (pembrolizumab) and stereotactic body radiotherapy doubled out-of-field responses[13]. Previous preclinical mouse studies with anti-CTLA4 and radiation identified PD-L1 as a common mechanism of resistance, which could be overcome with anti-PD-L1 therapy[14]. These promising early clinical trials and preclinical proof of concept led to this study of

combined dual blockade of PD-1 (nivolumab) and CTLA4 (ipilimumab) with radiation therapy in an attempt to stimulate immune responses in metastatic MSS CRC and PDAC.

# Results

### Efficacy of combined immune checkpoint inhibition and radiation

A total of 40 patients with CRC and 25 patients with PDAC were enrolled in this study (**Fig. 1**). All patients were confirmed MSS and had metastatic disease at enrollment. In the CRC cohort 18 were women and 22 men; median age, 59 years (range 26-83). 95% of patients were white, 65% had an ECOG performance status (PS) of 0, median number of prior treatments was 4 (range 1-13). The majority of patients (N=23, 58%) were metastatic at diagnosis and median time from diagnosis to cycle 1 day 1 was 44.9 months (**Table 1**). In the PDAC cohort 7 were women and 18 men; median age, 60 years (range 32-75). 92% of patients were white, 44% had an ECOG PS of 0, median number of prior treatments was 2 (range 1-4). The majority of patients (N=18, 72%) were locally advanced or metastatic at diagnosis and median time from diagnosis to cycle 1 day 1 was 16.9 months (**Table 1).**

In the 40 CRC patients who enrolled and started treatment, the disease control rate (DCR) was 25% (10/40) with an objective response rate (ORR) of 10% (4/40) by intention to treat (ITT) analysis. The CRC cohort had a median PFS of 2.4 months (95% CI: 1.8-2.5) and median OS of 7.1 months (95% CI: 4.3-10.9)(**Fig. 3 a, b**). Similarly, the 25 PDAC patients had a DCR of 20% (5/25) with an ORR of 12% (3/25) by ITT analysis. Median PFS was 2.5 months (95% CI: 1.6-2.8) with a median OS of 4.2 months (95% CI: 2.1-6.4)(**Fig. 3 a, b**). A total of 34 patients were treated with photons and 12 with protons. In both cohorts, 32% (CRC 13/40; PDAC 8/25) discontinued prior to radiation therapy given autoimmune toxicity leading to clinical decline (N=4), clinical progression (N=7), or progression confirmed by scans (N=10) (**Table 2** and **Supplementary Table 1**)**.**

Four patients in the per protocol group discontinued due to toxicity. In the CRC cohort adverse events (AEs) Grade $\geq$3 were reported in 83% of patients, 60% grade 3, 20% grade 4 and 3% grade 5. The most common Grade $\geq$3 AEs were lymphopenia, elevated lipase or amylase, anemia, diarrhea, colitis, hyponatremia, and fatigue, and the grade 5 toxicity was pneumonitis (**Table 3**). In the PDAC cohort AEs Grade $\geq$3 were reported in 60% of patients, 44% grade 3, 12% grade 4 and 4% grade 5. The most common Grade $\geq$3 AEs were lymphopenia, fatigue, hyperglycemia and elevated liver function tests, and the grade 5 toxicity was hepatic encephalopathy, possibly related to treatment (**Table 3**).

In a per protocol analysis of patients who received radiation therapy revealed the CRC cohort DCR was 37% (10/27) and ORR was 15% (4/27) and the PDAC cohort DCR was 29% (5/17) and ORR was 18% (3/17)**.** The Best Objective Response in CRC and PDAC are shown as a waterfall plot in **Fig. 2**. One CRC and one PDAC case had an impressive complete response (CR). The CRC cohort had a median PFS of 2.5 months (95% CI: 2.3-2.8) and median OS of 10.9 months (95% CI: 6.7-15.0) (**Fig. 3c, d**). Median PFS was

5.2 months (95% CI: 2.5-14.6) for the 10 patients with disease control as best overall response compared to 2.4 months (95% CI: 1.8-2.5) for the 17 without disease control. Median OS was 20.9 months (95% CI: 4.9-not reached) versus 7.7 months (95% CI: 4.0-11.3) for those with and without disease control. In the PDAC cohort, median PFS was 2.7 months (95% CI: 2.5-3.1) and median OS was 6.1 months (95% CI: 4.0-7.0) (**Fig. 3c, d**). Median PFS was 5.5 months (95% CI: 2.5-7.9) for the 5 patients with disease control as best overall response compared to 2.5 months (95% CI: 1.8-2.8) for the 12 without disease control. Median OS of the per-protocol cohort was 11.7 months (95% CI: 5.4-14.6) versus 4.4 months (95% CI: 3.6-6.4) for those with and without disease control respectively as their best overall response.

## Tumor mutational burden and coding gene mutation analysis

Patients underwent biopsies as able prior to trial initiation, immediately prior to radiation treatment, and after radiation completion. A total of 41 tumor samples with paired germline DNA from 17 patients from the per protocol cohort were analyzed by WES. All patients had low TMB with < 10 mutations/Mb (**Fig. 4a** and **Supplementary Table 2**), and there was no difference between patient non-responders (progressive disease = PD) compared to responders (stable disease = SD, partial response = PR, complete response = CR). Furthermore, there was no change in TMB before, during, or after treatment (**Fig. 4a**). Analysis of non-synonymous gene mutations identified expected genes that are frequently mutated including *KRAS* and *TP53* mutations in both CRC and PDAC, and common *APC* mutations in CRC (**Fig. 4b** and **Supplementary Tables 3 and 4**). In addition, there was notable mutations in DNA damage and repair pathway genes with shared frequent mutations in *DDX11* (CRC 4/13; PDAC 4/10) and *FANCD2* (CRC 2/13; PDAC 2/10). There was no specific DNA damage and repair pathway gene mutation that was particularly enriched in patients with response or disease stability. Notably, patient 4 (CRC PR) and patient 41 (PDAC CR) had 6 mutations in DNA damage and repair genes, which suggests a potential importance of these genes in predicting response, but there were not enough samples in this trial to make any clear conclusions.

## Repeat RNA expression and interferon response genes associated with disease control

A total of 32 samples from 13 patients who received radiation were analyzed by RNA-sequencing. Analysis of all biopsies comparing patients with disease control compared to progressive disease revealed 467 differentially expressed genes (FDR < 0.05) with 315 genes higher and 152 genes lower in responders compared to non-responders (**Fig. 5a** and **Supplementary Table 5**). Gene set enrichment of upregulated genes in responders noted enrichment of gene set HALLMARK_INTERFERON_GAMMA_RESPONSE (FDR = 4.11 E-05). Paired analysis of pre-radiation and post-radiation samples revealed 372 genes upregulated and 209 genes downregulated across all patients (FDR < 0.05; **Supplementary Table 6**). Interestingly, the most enriched gene set was again HALLMARK_INTERFERON_GAMMA_RESPONSE (FDR = 4.31E-25), which suggests an importance of

interferon gamma response genes in the biological activity of radiation induced immune response. Significant genes induced by radiation included multiple MHC Class I (*B2M*, *HLA-A*, *HLA-B*, *HLA-C*, *HLA-F*), MHC Class II (*HLA-DMA*, *HLA-DMB, HLA-DOA, HLA-DPA1, HLA-DPB1, HLA-DQA1, HLA-DRB1*), and inflammatory cytokines important in T-cell recruitment (*CXCL9*, *CXCL10*, *CCL5*), which indicates enhanced antigen presentation in radiated tumors (**Fig. 5b**). De-convolution of immune subsets in RNA-seq data using immune cell transcriptional signatures revealed a predominance of M2 (suppressive) macrophages and a paucity of CD8 T cells (**Supplementary Fig. 1**). While underpowered for this analysis, we observed a higher abundance of dendritic cells (DC) DCs in pre-radiation samples of responders compared to non-responders and an increased abundance of DCs overall after radiation that was more apparent in non-responders, which are trends that have been observed in pre-clinical models.[15] In addition, an increased NK and CD8 cell abundance was observed across all patients before treatment compared to after radiation, and a possible shift in the ratio of naive and memory CD4 T cells between pre- and post-radiation in responders and non-responders. Given the indication of a higher innate immune response in responders even in pretreatment samples, we analyzed RNA-seq for expression levels of repeat element RNAs, a class of transcripts that have been shown to be linked with activation of innate immune receptors and an interferon response in other cancers and model systems[16-20]. Strikingly, we found aberrantly high levels of 147 repeat RNAs in responders compared to non-responders, and only 9 repeat RNAs lower in responders compared to non-responders (**Fig. 5c** and **Supplementary Table 7**). Analysis of major repeat elements identified significantly higher expression of the HERV-K endogenous retrovirus in patients with disease control compared to progressors ($p < 0.0001$; **Fig. 5d**). Altogether, the de-repression of repeat elements linked with dysregulated interferon response is associated with disease control and response in patients who received radiation with combined immune checkpoint blockade.

# Discussion

This is a proof-of-concept study demonstrating the safety and efficacy of radiation therapy to enhance the effects of dual checkpoint inhibition in MSS metastatic CRC and PDAC. Responses were observed in the group of patients who were able to receive radiation therapy and this contributes to the growing prospective data suggesting radiation therapy may enhance the response rate of immunotherapy[13]. However, what is most notable is the duration of disease control in the patients who had either responses or stable disease. This suggests that using overall response rate to determine efficacy for immunotherapy treatment may perhaps underappreciate the benefit in patients. However, though not directly comparable, the response rate with ipilimumab, nivolumab, and radiation combination still surpasses the single-digit response rates seen with regorafenib or trifluridine and tipiracil in CRC or gemcitabine after FOLFIRINOX in PDAC[21–23]. Toxicity rates in both cohorts were high, but only a small number of patients stopped treatment given toxicity, indicating that toxicity was not limiting and manageable. There was one CRC patient with grade 5 pneumonitis, but this patient also had a substantial degree of underlying lung disease which may have also been contributory and in the PDAC cohort there was one grade 5 hepatic encephalopathy in a patient with extensive liver disease with concomitant hepatotoxicity from immunotherapy.

There was notable early dropout (progression, toxicity, declining PS) in this trial as a third of patients in both cohorts never had the opportunity to receive radiation. Alternative dosing schedules for the integration of radiation with immunotherapy might be more active as the extent of immune-modulation with varying dosing and fractionating radiation therapy is still not well understood and continues to be under investigation[24–26]. For example, recent data suggests that PD-1 blockade prior to antigen priming leads to T-cell exhaustion given the induction of dysfunctional $CD8^+$ cells by PD-1 blockade.[27] Therefore, concurrent priming may be optimal in preventing the induction of dysfunctional CD8 cells and the sequencing in this study (with anti-PD1 therapy given for 3 doses before radiation therapy was delivered) may have been suboptimal. In the future, it will be critical to consider modifications to the dosing schedule to accommodate radiation upfront as well as modifications that mitigate the toxicity seen.

Although the exact mechanism for response from this approach is not fully understood, preclinical models have indicated that radiation enhances the diversity of T-cell receptor (TCR) repertoire in intratumoral T-cells and increases dendritic cell infiltration and antigen presentation in the tumor[14,24,28–30]. Our analysis of pre and post radiation biopsies is consistent with the increased expression of antigen presentation genes and dendritic cell infiltrates, which indicates that dual immune checkpoint blockade and radiation therapy can alter myeloid and lymphoid subsets; however, these results will need to be confirmed in larger studies. Analysis of biopsies for potential genomic predictive biomarkers of response noted all tumors had low TMB and there were no clear mutations associated with response. Although a couple of patients with response had tumors with multiple mutations in DNA damage and repair pathway genes, there was no consistent pattern of response as has been recently demonstrated in a larger series of tumors treated by immune checkpoint inhibitors[31]. Analysis of the transcriptome demonstrated significant expression of multiple repeat RNAs with concordant elevation of interferon response genes in patients with disease control or response. These findings are consistent with previous reports showing a relationship of repeat RNA expression and response to immune checkpoint inhibitors[18,32]. Although there are multiple repeat RNAs elevated in pancreatic and colorectal cancers that responded to therapy, there appears to be clear distinct expression pattern of this wide spectrum of repeat RNAs that are associated with different epigenetic and immunologic features of these cancers[32–34]. For example, the specific elevation of the endogenous retrovirus HERV-K in responders is consistent with our previously reported correlation of this particular repeat RNA with immune checkpoint response in urothelial carcinoma. [32] Altogether, this indicates that specific repeat RNAs are likely associated with differences in innate immune response and infiltrating immune cells that can be used as potential predictive biomarkers of modified immune checkpoint inhibitor trials. The functional relationship of these repeat RNAs on innate immune sensing pathways and associated immune cell response is an underdeveloped area of research that merits further investigation.

The addition of radiation therapy to PD-1 and CTLA4 pathway inhibition has activity in otherwise refractory CRC and PDAC patients for whom dual PD-1 and CTLA4 pathway inhibition historically has had limited activity. Though modest, duration of disease control and clinical benefit was notable in this human proof of concept study, warranting further investigation in a confirmatory study. Furthermore,

given the high level of early-drop out in this trial as well as new information on potential improved timing of the sequencing of radiation therapy with immunotherapy to enhance efficacy, follow up studies with a different treatment schedule, including moving the radiation treatment to earlier in the treatment course, are planned. Moreover, repeat RNA and interferon response gene expression profiling can serve as a potential predictive biomarker of response and be used as a future inclusion criterion for these trial concepts.

# Declarations

### Data Availability Statement

All RNA-seq data and whole exome sequencing will be uploaded to NCBI GEO and SRA before publication.

### Code Availability Statement

There was no custom code or mathematical algorithm used for this work.


### Acknowledgements

Research support from SU2C-AACR-DT22-17 Colorectal Dream Team: Targeting Genomic, Metabolic, and Immunological Vulnerabilities of Colorectal Cancer, P50CA127003 DF/HCC SPORE in Gastrointestinal Cancer, Conquer Cancer Foundation ASCO CDA, SU2C and Lustgarten Foundation, and generous donations from David and Ingrid Kosowsky, and Sandra and Arthur Irving.


### Disclosure of Potential Conflicts of Interest

A.R.P is a consultant/advisory board member for Eli Lilly and Natera. Institutional research funding from Eli Lilly, Array, Plexxikon, Guardant, BMS, Novartis, Tesaro, and Macrogenics.

T.S.H. is consultant/advisory board member for Merck, E Serono, and Synthetic Biologics; research support from Taiho, Astra Zeneca, Bristol Myers Squibb, Mobetron, and Ipsen.

D.T.T. has received consulting fees from Pfizer, ROME therapeutics, Merrimack Pharmaceuticals, Ventana Roche, Nanostring Technologies, Inc., Foundation Medicine, Inc., and EMD Millipore Sigma, which are not

related to this work. D.T.T. is a founder and has equity in PanTher Therapeutics, ROME therapeutics, and TellBio, Inc., which are not related to this work. D.T.T. receives research funding from ACD-Biotechne, PureTech Health LLC, and Ribon Therapeutics, which was not used in this work. D.T.T.'s interests were reviewed and are managed by Massachusetts General Hospital and Mass General Brigham in accordance with their conflict of interest policies.

L.G. is a consultant or advisory board member for Debiopharm, H3 Biomedicine, Agios Pharmaceuticals, Taiho Pharmaceuticals, Klus Pharmaceuticals, QED, Alentis Pharmaceuticals, and Pieris Pharmaceuticals.

A.X.Z is a consultant/ advisor for AstraZeneca, Bayer, Bristol-Myers Squibb, Eisai, Eli Lilly, Exelixis, Merck, Novartis, and Roche/Genentech; research funding from Bayer, Bristol-Myers Squibb, Eli Lilly, Merck, and Novartis. N.H. is a founder and SAB member of Neon Therapeutics.

D.P.R. serves on advisory board for MPM Capital, Gritstone Oncology, Oncorus, Maverick Therapeutics, 28/7 Therapeutics; has equity in MPM Capital and Acworth Pharmaceuticals; serves as author for Johns Hopkins University Press, UpToDate, McGraw Hill.

R.B.C. is a consultant/advisory board member for Amgen, Array Biopharma, Astex Pharmaceuticals, Avidity Biosciences, BMS, C4 Therapeutics, Chugai, Elicio, Fog Pharma, Kinnate Biopharma, Genentech, LOXO, Merrimack, N-of-one, Novartis, nRichDx, Revolution Medicines, Roche, Roivant, Shionogi, Shire, Spectrum Pharmaceuticals, Symphogen, Taiho, and Warp Drive Bio; holds equity in Avidity Biosciences, C4 Therapeutics, Kinnate Biopharma, nRichDx, and Revolution Medicines; and has received research funding from Asana, AstraZeneca, and Sanofı.

All other authors have no disclosures.

# References

1. https://www.cancer.org/cancer/colon-rectal-cancer/about/key-statistics.html. Accessed June 17, 2019.
2. Conroy T, Desseigne F, Ychou M, et al. FOLFIRINOX versus gemcitabine for metastatic pancreatic cancer. *N Engl J Med.* 2011;364(19):1817-1825.
3. Le DT, Durham JN, Smith KN, et al. Mismatch-repair deficiency predicts response of solid tumors to PD-1 blockade. *Science (New York, NY).* 2017;357(6349):409-413.
4. Chung KY, Gore I, Fong L, et al. Phase II study of the anti-cytotoxic T-lymphocyte-associated antigen 4 monoclonal antibody, tremelimumab, in patients with refractory metastatic colorectal cancer. *J Clin Oncol.* 2010;28(21):3485-3490.
5. O'Reilly EM, Oh DY, Dhani N, et al. Durvalumab With or Without Tremelimumab for Patients With Metastatic Pancreatic Ductal Adenocarcinoma: A Phase 2 Randomized Clinical Trial. *JAMA Oncol.* 2019.
6. Chen EX, Jonker DJ, Loree JM, et al. Effect of Combined Immune Checkpoint Inhibition vs Best Supportive Care Alone in Patients With Advanced Colorectal Cancer: The Canadian Cancer Trials Group CO.26 Study. *JAMA Oncology.* 2020;6(6):831-838.
7. Le DT, Uram JN, Wang H, et al. PD-1 Blockade in Tumors with Mismatch-Repair Deficiency. *New England Journal of Medicine.* 2015;372(26):2509-2520.
8. Marabelle A, Le DT, Ascierto PA, et al. Efficacy of Pembrolizumab in Patients With Noncolorectal High Microsatellite Instability/Mismatch Repair-Deficient Cancer: Results From the Phase II KEYNOTE-158 Study. *J Clin Oncol.* 2020;38(1):1-10.
9. Hu ZI, Shia J, Stadler ZK, et al. Evaluating Mismatch Repair Deficiency in Pancreatic Adenocarcinoma: Challenges and Recommendations. *Clin Cancer Res.* 2018;24(6):1326-1336.
10. Jiang W, Chan CK, Weissman IL, Kim BYS, Hahn SM. Immune Priming of the Tumor Microenvironment by Radiation. *Trends in cancer.* 2016;2(11):638-645.
11. Deng L, Liang H, Burnette B, et al. Irradiation and anti-PD-L1 treatment synergistically promote antitumor immunity in mice. *The Journal of clinical investigation.* 2014;124(2):687-695.
12. Formenti SC, Rudqvist NP, Golden E, et al. Radiotherapy induces responses of lung cancer to CTLA-4 blockade. *Nature medicine.* 2018;24(12):1845-1851.
13. Theelen WSME, Peulen HMU, Lalezari F, et al. Effect of Pembrolizumab After Stereotactic Body Radiotherapy vs Pembrolizumab Alone on Tumor Response in Patients With Advanced Non–Small Cell Lung Cancer: Results of the PEMBRO-RT Phase 2 Randomized Clinical TrialPembrolizumab Alone vs After Stereotactic Body Radiotherapy in Patients With Advanced NSCLCPembrolizumab Alone vs After Stereotactic Body Radiotherapy in Patients With Advanced NSCLC. *JAMA Oncology.* 2019.
14. Twyman-Saint Victor C, Rech AJ, Maity A, et al. Radiation and dual checkpoint blockade activate non-redundant immune mechanisms in cancer. *Nature.* 2015;520(7547):373-377.
15. Hegde S, Krisnawan VE, Herzog BH, et al. Dendritic Cell Paucity Leads to Dysfunctional Immune Surveillance in Pancreatic Cancer. *Cancer Cell.* 2020;37(3):289-307.e289.

16. Tanne A, Muniz LR, Puzio-Kuter A, et al. Distinguishing the immunostimulatory properties of noncoding RNAs expressed in cancer cells. *Proceedings of the National Academy of Sciences.* 2015;112(49):15154-15159.
17. Leonova KI, Brodsky L, Lipchick B, et al. p53 cooperates with DNA methylation and a suicidal interferon response to maintain epigenetic silencing of repeats and noncoding RNAs. *Proceedings of the National Academy of Sciences.* 2013;110(1):E89-E98.
18. Chiappinelli KB, Strissel PL, Desrichard A, et al. Inhibiting DNA Methylation Causes an Interferon Response in Cancer via dsRNA Including Endogenous Retroviruses. *Cell.* 2015;162(5):974-986.
19. Roulois D, Loo Yau H, Singhania R, et al. DNA-Demethylating Agents Target Colorectal Cancer Cells by Inducing Viral Mimicry by Endogenous Transcripts. *Cell.* 2015;162(5):961-973.
20. Cañadas I, Thummalapalli R, Kim JW, et al. Tumor innate immunity primed by specific interferon-stimulated endogenous retroviruses. *Nat Med.* 2018;24(8):1143-1150.
21. Grothey A, Van Cutsem E, Sobrero A, et al. Regorafenib monotherapy for previously treated metastatic colorectal cancer (CORRECT): an international, multicentre, randomised, placebo-controlled, phase 3 trial. *Lancet (London, England).* 2013;381(9863):303-312.
22. Mayer RJ, Van Cutsem E, Falcone A, et al. Randomized trial of TAS-102 for refractory metastatic colorectal cancer. *N Engl J Med.* 2015;372(20):1909-1919.
23. Gilabert M, Chanez B, Rho YS, et al. Evaluation of gemcitabine efficacy after the FOLFIRINOX regimen in patients with advanced pancreatic adenocarcinoma. *Medicine (Baltimore).* 2017;96(16):e6544.
24. Dewan MZ, Galloway AE, Kawashima N, et al. Fractionated but not single-dose radiotherapy induces an immune-mediated abscopal effect when combined with anti-CTLA-4 antibody. *Clin Cancer Res.* 2009;15(17):5379-5388.
25. Demaria S, Formenti SC. Radiation as an immunological adjuvant: current evidence on dose and fractionation. *Frontiers in oncology.* 2012;2:153.
26. Schaue D, Ratikan JA, Iwamoto KS, McBride WH. Maximizing tumor immunity with fractionated radiation. *International journal of radiation oncology, biology, physics.* 2012;83(4):1306-1310.
27. Verma V, Shrimali RK, Ahmad S, et al. PD-1 blockade in subprimed CD8 cells induces dysfunctional PD-1(+)CD38(hi) cells and anti-PD-1 resistance. *Nat Immunol.* 2019.
28. Rodriguez-Ruiz ME, Vitale I, Harrington KJ, Melero I, Galluzzi L. Immunological impact of cell death signaling driven by radiation on the tumor microenvironment. *Nature Immunology.* 2020;21(2):120-134.
29. Hindson J. Radiation promotes systemic responses. *Nature Reviews Immunology.* 2019;19(1):3-3.
30. Dovedi SJ, Cheadle EJ, Popple AL, et al. Fractionated Radiation Therapy Stimulates Antitumor Immunity Mediated by Both Resident and Infiltrating Polyclonal T-cell Populations when Combined with PD-1 Blockade. *Clin Cancer Res.* 2017;23(18):5514-5526.

31. Hsiehchen D, Hsieh A, Samstein RM, et al. DNA Repair Gene Mutations as Predictors of Immune Checkpoint Inhibitor Response beyond Tumor Mutation Burden. *Cell Reports Medicine.* 2020;1(3):100034.
32. Solovyov A, Vabret N, Arora KS, et al. Global Cancer Transcriptome Quantifies Repeat Element Polarization between Immunotherapy Responsive and T Cell Suppressive Classes. *Cell Reports.* 2018;23(2):512-521.
33. Ting DT, Lipson D, Paul S, et al. Aberrant overexpression of satellite repeats in pancreatic and other epithelial cancers. *Science.* 2011;331(6017):593-596.
34. Desai N, Sajed D, Arora KS, et al. Diverse repetitive element RNA expression defines epigenetic and immunologic features of colon cancer. *JCI Insight.* 2017;2(3).
35. World Medical Association Declaration of Helsinki: ethical principles for medical research involving human subjects. *Jama.* 2013;310(20):2191-2194.
36. Eisenhauer EA, Therasse P, Bogaerts J, et al. New response evaluation criteria in solid tumours: revised RECIST guideline (version 1.1). *European journal of cancer (Oxford, England : 1990).* 2009;45(2):228-247.

# Methods

**Trial Registration:** Nivolumab and Ipilimumab and Radiation Therapy in Microsatellite Stable (MSS) and Microsatellite Instability (MSI) High Colorectal and Pancreatic Cancer**.** Registration **#**NCT03104439. https://clinicaltrials.gov/ct2/show/NCT03104439?term=17-021&rank=1.

### Patient Selection

*Metastatic MSS Colorectal Cancer*

Eligibility criteria included; at least 18 years old; histologically or cytologically confirmed adenocarcinoma of colorectal documented as MSS by PCR and/or IHC; Eastern Cooperative Oncology Group performance status £1; life expectancy of greater than 3 months; adequate hematologic function (absolute neutrophil count ³1000/mcL, white blood count ³2000/mcL, platelets ³75,000/mcL, hemoglobin ³7.5 g/dL); adequate renal function (serum creatinine £1.5 the upper limit of normal or creatinine clearance ³ 40ml/min); adequate hepatic function (serum total bilirubin £1.5 the upper limit of normal, AST and ALT £3 the upper limit of normal or £ 5 the upper limit of normal in patients with liver metastases; adequate coagulation (International Normalized Ratio or Prothrombin Time (PT) ≤1.5 X ULN and Activated Partial Thromboplastin Time (aPTT) ≤2.5 X ULN; participants must have been on a stable dose of dexamethasone 2 mg or less for 7 days prior to initiation of treatment. Participants were also required to have one previously unirradiated lesion to serve as the radiotherapy target lesion amenable to a prescribed dose of 8 Gy x 3 which would meet dose constraints, and another unirradiated measurable lesion > 1 cm in size outside the radiation field that could be used as measurable disease; documentation

of microsatellite status; patients must have received prior fluorouracil (5FU), irinotecan and oxaliplatin (any combination) or have a contraindication to receiving these agents.

Exclusion criteria include participants who had received chemotherapy, targeted small molecule therapy or study therapy within 14 days of protocol treatment, or those who have not recovered [i.e., ≤ Grade 1 (or ≤ Grade 2 for neuropathy) or at baseline] from adverse events due to agents administered more than 2 weeks earlier. Subjects with major surgery must have recovered adequately; participants currently receiving any other investigational agents; known or suspected autoimmune disease other than vitiligo, type I diabetes mellitus, residual hypothyroidism due to autoimmune condition only requiring hormone replacement, psoriasis not requiring systemic treatment, or conditions not expected to recur in the absence of an external trigger condition requiring systemic treatment with either corticosteroids (> 10 mg daily prednisone equivalents) or other immunosuppressive medications within 14 days of study drug administration); prior systemic treatment with an anti-CTLA4 antibody, anti-PD1 or PDL1 antibody; known history of active TB, HBV, HCV or HIV; uncontrolled intercurrent illness or psychiatric illness/social situations that would limit compliance with study requirements; pregnant or breastfeeding; known additional malignancy that is progressing or requires active treatment (excluding basal cell carcinoma of the skin and squamous cell carcinoma of the skin that has undergone potentially curative therapy or in situ cervical cancer); known history of, or any evidence of active, non-infectious pneumonitis; active infection requiring systemic therapy; received a live vaccine within 30 days of planned start of study therapy; history of allergy to study drug components; history of severe hypersensitivity reaction to any monoclonal antibody; uncontrolled brain metastases (patients treated with radiation ≥ 4 weeks prior with follow up imaging showing control were eligible).

*Metastatic MSS Pancreatic Ductal Adenocarcinoma*

Inclusion criteria was identical to MSS CRC cohort except for the following differences: histologically or cytologically confirmed adenocarcinoma of pancreas, patients could receive treatment after progressing on one or more lines of therapy, and documentation of microsatellite status was required but did not preclude eligibility.

Exclusion criteria also were identical to the MSS cohort of included participants except in the PDAC cohort, patients could have received prior PD-1 or PDL-1 inhibitors.

The trial protocol is provided in Supplement 1. All procedures were conducted in accordance with the Declaration of Helsinki and the International Conference on Harmonization Guidelines for Good Clinical Practice.[35] The protocol and all amendments were reviewed by the scientific review committee and institutional review board at the Dana Farber Cancer Institute/Harvard Cancer Center. All patients provided written informed consent prior to enrollment.

## Study Design and Treatment

This was an open-label, single-arm, Phase 2 clinical trial conducted at the Massachusetts General Hospital (MGH) Cancer Center in Boston, MA. Patients enrolled between 07/2017 to 12/2018. On cycle 1, day 1, patients received one dose of nivolumab 240 mg and ipilimumab 1 mg/kg. Nivolumab was administered first as a 30-minute IV infusion followed by ipilimumab, as a 30-min IV infusion, 30 minutes after completion of the nivolumab infusion. Patients went on to receive nivolumab 240 mg once every two weeks, on days 15, 29 of a 42-day cycle. On cycle 2, day 1, patients again received nivolumab 240 mg and ipilimumab 1 mg/kg but also started radiation. Patients received 24 Gy total given as 3 fractions of 8 Gy administered every other day or 2 days as needed. All treatments were administered at either the Clark Center for Radiation Oncology or the Francis H. Burr Proton Center at MGH. After radiation, treatment continued with receive nivolumab 240 mg days every two weeks, on days 15, 29 of a 42-day cycle. For cycle 3 and beyond, patients continued treatment with ipilimumab 1 mg/kg on day 1 with nivolumab 240 mg and then nivolumab every two weeks for a 42 day cycle until disease progression defined according to Response Evaluation Criteria in Solid Tumors version 1.1[36], unacceptable toxicity, or withdrawal. Dose interruptions and management of immunologic toxicities were in accordance with the protocol.

## Correlative Science

Optional biopsies of the tumor site being radiated were done prior to treatment, immediately prior to radiation (weeks 2-5) and within 2 weeks after radiation completion. Whole blood was obtained from patients for DNA germline control. RNA and genomic DNA was extracted from fresh frozen biopsies after homogenization with a TissueLyser (2x4 minutes at 20Hz), using the Qiagen AllPrep DNA/RNA/Protein mini kit (Cat.No.80004, Qiagen) according to manufacturer instructions. Germline genomic DNA was extracted from whole blood samples with the use of the DNAzol BD reagent (10974020, Invitrogen).

### *Whole Exome Sequencing (WES)*

A total of 41 tumor samples with paired germline DNA from 17 patients from the per protocol cohort were analyzed by WES. The Nextera DNA Exome kit (20020617, Illumina) was used to prepare pooled libraries enriched in exonic regions. A genomic DNA input of 50 ng was used per sample. After library preparation and amplification (10 cycles), up to 8 dual indexed libraries were pooled together for the downstream enrichment steps. Pooled samples were sequenced using on a HiSeq X using 150-150 paired end reads.

### *Whole Exome Sequencing analysis*

We called single nucleotide variations (SNVs) and indel mutations from paired-end whole-exome sequencing reads, for which read lengths were 150 base pairs. We downloaded the Broad Institute's GATK b37 resource bundle [1] as reference data for read processing. We pre-processed sequencing reads according to GATK Best Practices recommendations [2, 3].

We first aligned the sequencing reads to the human_g1k_v37_decoy reference genome (GRCh37) using bwa-0.7.17 mem [4] and samtools-1.6 [5]. Duplicates were marked with picard-2.11.0 MarkDuplicates [6]. Indel realignments were done with the Genome Analysis toolkit (GenomeAnalysisTK-3.8-1-0-gf15c1c3ef) RealignerTargetCreator and IndelRealigner [7] using the 1000 genome phase1 indel (1000G_phase1.indels.b37.vcf) and Mills indel calls (Mills_and_1000G_gold_standard.indels.b37.vcf) as references. Base calls were recalibrated with BaseRecalibrator [7] and dbSNP version 138.

MuTect 1.1.7 [8] and Strelka 1.0.15 [9] were used to call SNVs and indels on pre-processed sequencing data. For the MuTect calls, dbSNP 138 and CosmicCodingMuts.vcf version 86 [10] were used as reference files. For the Strelka calls, we set “isSkipDepthFilters = 1” to prevent filtering-out of mutation calls from exome sequencing due to exome-sequencing mapping breadth.

Unbiased normal/tumor read counts for each SNV and indel call were then assigned with the bam-readcount software (0.8.0-unstable-6-963acab-dirty (commit 963acab-dirty)) [11]. A minimum base quality filter of “-b 15” was used for all mutations except for possible KRAS mutations, which instead had no such filter. This was to capture all possible driver KRAS mutations. The reads were counted in an insertion-centric way with the “-i” flag, so that reads overlapping with insertions were not included in the per-base read counts. of The union of all mutation calls were annotated with the snpEff.v4.3t software [12] using the following code:

```
$java_path -jar $snpeff_path ann \
   -noStats \
   -strict \
   -hgvs1LetterAa \
   -hgvs \
   -canon \
   -fastaProt $output_path/"$vcf_name"".fasta" \
   GRCh37.75 \
   $input_vcf \
```

> $output_path/"$vcf_name""_ann.vcf"

Only annotations without “WARNING” or “ERROR” were kept.

Common mutations in KRAS known to be pathogenic were then manually curated (chromosome 12, bases 25378562, 25380275, 25398281, 25398282, 25398284, and 25398285) corresponding to the top ten coding mutations in KRAS denoted in the Genomic Data Commons Database [13] if the sample already did not already contain a KRAS mutation. Five additional KRAS mutations were added in this way.

Tumor mutational burden (TMB) was computed for: (1) all mutations, (2) nonsynonymous SNV mutations, and (3) missense mutations. Coding mutations with variant allele frequencies greater than 10% were reported as “high-quality”. All KRAS mutations were reported.

[1] https://gatk.broadinstitute.org/hc/en-us/articles/360035890811-Resource-bundle

[2] DePristo MA, Banks E, Poplin R, Garimella KV, Maguire JR, Hartl C, Philippakis AA, Del Angel G, Rivas MA, Hanna M, McKenna A. A framework for variation discovery and genotyping using next-generation DNA sequencing data. Nature genetics. 2011 May;43(5):491.

[3] Van der Auwera GA, Carneiro MO, Hartl C, Poplin R, Del Angel G, Levy-Moonshine A, Jordan T, Shakir K, Roazen D, Thibault J, Banks E. From FastQ data to high-confidence variant calls: the genome analysis toolkit best practices pipeline. Current protocols in bioinformatics. 2013 Oct;43(1):11-0.

[4] Li H. Aligning sequence reads, clone sequences and assembly contigs with BWA-MEM. arXiv preprint arXiv:1303.3997. 2013 Mar 16.

[5] Li H, Handsaker B, Wysoker A, Fennell T, Ruan J, Homer N, Marth G, Abecasis G, Durbin R. The sequence alignment/map format and SAMtools. Bioinformatics. 2009 Aug 15;25(16):2078-9.

[6] http://broadinstitute.github.io/picard

[7] McKenna A, Hanna M, Banks E, Sivachenko A, Cibulskis K, Kernytsky A, Garimella K, Altshuler D, Gabriel S, Daly M, DePristo MA. The Genome Analysis Toolkit: a MapReduce framework for analyzing next-generation DNA sequencing data. Genome research. 2010 Sep 1;20(9):1297-303.

[8] Cibulskis K, Lawrence MS, Carter SL, Sivachenko A, Jaffe D, Sougnez C, Gabriel S, Meyerson M, Lander ES, Getz G. Sensitive detection of somatic point mutations in impure and heterogeneous cancer samples. Nature biotechnology. 2013 Mar;31(3):213-9.

[9] Saunders CT, Wong WS, Swamy S, Becq J, Murray LJ, Cheetham RK. Strelka: accurate somatic small-variant calling from sequenced tumor–normal sample pairs. Bioinformatics. 2012 Jul 15;28(14):1811-7.

[10] Tate JG, Bamford S, Jubb HC, Sondka Z, Beare DM, Bindal N, Boutselakis H, Cole CG, Creatore C, Dawson E, Fish P. COSMIC: the catalogue of somatic mutations in cancer. Nucleic acids research. 2019 Jan 8;47(D1):D941-7.

[11] https://github.com/genome/bam-readcount

[12] Cingolani P, Platts A, Wang LL, Coon M, Nguyen T, Wang L, Land SJ, Lu X, Ruden DM. A program for annotating and predicting the effects of single nucleotide polymorphisms, SnpEff: SNPs in the genome of Drosophila melanogaster strain w1118; iso-2; iso-3. Fly. 2012 Apr 1;6(2):80-92.

[13] Grossman RL, Heath AP, Ferretti V, Varmus HE, Lowy DR, Kibbe WA, Staudt LM. Toward a shared vision for cancer genomic data. New England Journal of Medicine. 2016 Sep 22;375(12):1109-12.

*Total RNA sequencing (RNA-seq)*

The Smarter Stranded Total RNA-Seq kit v2 (634413, Takara) was used with 10 ng RNA input and 4 minutes fragmentation time, according to the manufacturer instructions to generate dual-indexed libraries for total RNA sequencing. After qPCR-based quantification (KAPA library quantification kit, 07960140001, Roche), libraries were pooled and sequenced on the Illumina NextSeq 500 platform using a 150 cycles kit with paired end read mode.

*RNA-seq computational analysis*

Raw Illumina reads were quality-filtered as follows. First, ends of the reads were trimmed to remove N's and bases with quality less than 20. After that, the quality scores of the remaining bases were sorted, and the quality at the 20th percentile was computed. If the quality at the 20th percentile was less than 15, the whole read was discarded. Also, reads shorter than 40 bases after trimming were discarded. If at least one of the reads in the pair failed the quality check and had to be discarded, we discarded the mate as well.

Quality filtered reads were mapped to the human genome (gencode annotation, build 38) and to repbase elements (release 20) using STAR aligner. Aligned reads were assigned to genes using the featureCounts function of the Rsubread package using the external Ensembl annotation. This produced the raw read counts for each gene. Mapping and counting of the reads was done in 2 stages. First, reads were mapped to the human genome, and the counts were determined using the Gencode annotation and the annotation derived from the repeatmasker output. After that, the reads which were not assigned to any feature in either Gencode and repeatmasker annotation were realigned to the repeat consensus sequence (repbase). Counts obtained from repeatmasker and repbase were added together.

*Differential Gene Expression Analysis*

Differential expression and statistical analysis were performed using DESeq2 in R, with un-normalized raw read counts as the input. A false discovery rate (FDR) adjusted p value < 0.05 was used for the selection of differentially expressed genes. Before plotting, repeat RNA was normalized to total protein coding counts, and protein coding genes were RPM normalized.

## Assessments

Participants were seen weekly for clinical assessments including a physical examination with vital signs, performance status, hematology, and biochemistry tests on or within 72 hours before Day 1, then weekly until week 12, and subsequently every two weeks. Participants were evaluated for radiographic response every 12 weeks, noting that the first scan was performed after completion of radiation. In

addition to a baseline scan, confirmatory scans were obtained 3 weeks following initial documentation of objective response. Scans could also be obtained prior to every 12 weeks at the clinician's request. Patients were followed for survival until death, withdrawal of consent for follow-up or up to 5 years. All AEs were monitored from registration until 30 days after treatment and were graded according to the National Cancer Institute Common Terminology Criteria for Adverse Events, Version 4.03. Following disease progression, patients were followed-up within 30 days from the last dose +/- 7 days or coinciding with the date of discontinuation (+/- 7 days) if date of discontinuation was greater than 37 days after last dose with a second follow-up visit 8-10 weeks (+/- 7 days) from follow-up visit 1. After 2 in person follow-up visits, patients were followed with a phone call or in clinic visit every 10-12 weeks for survival.

### Study End Points

The primary trial endpoint was disease control rate (response plus stable disease [DCR]) by RECIST 1.1. Responses and stable disease were defined as responses and stability outside of the irradiated field. Secondary endpoints include overall response rate (complete response and partial response [ORR]) in unirradiated lesions, treatment-related adverse event (AE) rates, overall survival (OS) and progression-free survival (PFS). Exploratory objectives included biomarker analysis of serial tumor biopsies and peripheral blood samples.

### Statistical Analysis

A two-stage design was used to demonstrate a DCR of 20% under the alternative hypothesis as the minimum level of promising efficacy, while a 5% rate is specified under the null hypothesis to indicate minimal or no activity. In the MSS cohort if at least 2 of the first 20 patients achieved disease control, the cohort proceeded to enroll a total of 40 patients. The two-stage design provided 92% power to accept the protocol treatment is associated with a 20% rate of disease control, while the probability of a type 1 error is 10% if the underlying rate of disease control were truly only 5%. In the mPDAC cohort if at least 1 of the first 15 patients achieved disease control, the cohort proceeded to enroll a total of 25 patients. The two-stage design provided 89% power to accept the protocol treatment is associated with a DCR of 20%, while the probability of a type 1 error is 12% if the underlying DCR were truly only 5%. PFS and OS were measured from the first dose of protocol treatment. PFS was defined as time until the earlier date of either progressive disease or death, or otherwise censored at the date of last follow-up. OS was defined as time to death from any cause or otherwise censored at the date of last follow-up for patients still alive at the time of analysis. OS and PFS curves were estimated by the Kaplan-Meier method, with the 95% confidence interval (95% CI) obtained by the log-log transformation. Analyses were done for the intention-to-treat (ITT) population as well as the per protocol analysis, defined as patients who received radiation. Statistical analyses were performed using SAS version 9.4 (SAS Institute, Cary, NC) and R version 3.3.1 (R Foundation).

# Tables

**Table 1. Baseline patient and disease characteristics**

| Baseline Patient and Disease Characteristics | | |
|---|---|---|
| | **Colorectal** | **Pancreas** |
| Characteristic | N = 40 | N = 25 |
| Median age, years (range) | 59 (26-83) | 60 (32-75) |
| Race<br>White<br>Black/Asian/Other | 38 (95%)<br>2 (5%) | 23 (92%)<br>2 (8%) |
| Male Sex | 22 (55%) | 18 (72%) |
| ECOG PS<br>0<br>1 | 26 (65%)<br>14 (35%) | 11 (44%)<br>14 (56%) |
| Median Number of Prior Regimens (including Chemotherapy and ChemoRT) (range) | 4 (1-13) | 2 (1-4) |
| Stage at Diagnosis<br>Upfront Resectable<br>Borderline *(PDAC only)*<br>Locally Advanced *(PDAC only)*<br>Metastatic | <br>17 (42%)<br>N/A<br>N/A<br>23 (58%) | <br>6 (24%)<br>1 (4%)<br>7 (28%)<br>11 (44%) |
| Median Time from Diagnosis to C1D1 (Months) (range) | 44.9 (7.2-198.7) | 16.9 (3.7-54.8) |

**Table 2. Efficacy by best overall response**

| Efficacy | | | | |
|---|---|---|---|---|
| | Colorectal | | Pancreas | |
| | ITT (N=40) | Per Protocol (N=27) | ITT (n=25) | Per Protocol (n=17) |
| ORR | 4 (10%) | 4 (15%) | 3 (12%) | 3 (18%) |
| DCR | 10 (25%) | 10 (37%) | 5 (20%) | 5 (29%) |
| Discontinued due to toxicity[a,b] | 4 (10%) | 1 (4%) | 1 (4%) | 1 (6%) |
| Progression free survival (median in months) | 2.4 | 2.5 | 2.5 | 2.7 |
| Overall survival (median in months)[c] | 7.1 | 10.9 | 4.2 | 6.1 |

a. Colorectal cohort discontinuation prior to xRT: toxicity (4), progression confirmed by scans (6), clinical progression (3)
b. Pancreas cohort discontinuation prior to xRT: toxicity (0), progression confirmed by scans (4), clinical progression (4)
c. Colorectal cohort: 6 patients alive with median follow-up of 16.6 months (range 5.4-28.0); Pancreas cohort: 1 patient alive at 13.9 months

**Treatment-related adverse events, worse grade per patient**

| Treatment-related adverse events, worst grade by patient | | | | | | |
|---|---|---|---|---|---|---|
| | Colorectal | | | Pancreas | | |
| | Grade 3 | Grade 4 | Grades 3-5 | Grade 3 | Grade 4 | Grades 3-5 |
| Lymphopenia | 10 (25%) | 2 (5.0%) | 12 (30%) | 5 (20%) | 1 (4.0%) | 6 (24%) |
| Leukopenia | 0 | 0 | 0 | 1 (4.0%) | 0 | 1 (4.0%) |
| Anemia | 5 (13%) | 0 | 5 (13%) | 2 (8.0%) | 0 | 2 (8.0%) |
| Fatigue | 4 (10%) | 0 | 4 (10%) | 4 (10%) | 0 | 4 (10%) |
| Hyperlipasemia/Hyperamylasemia | 2 (5.0%) | 3 (7.5%) | 5 (13%) | 0 | 2 (8.0%) | 2 (8.0%) |
| Pancreatitis | 2 (5.0%) | 0 | 2 (5.0%) | 0 | 0 | 0 |
| Diarrhea | 4 (10%) | 0 | 4 (10%) | 1 (4.0%) | 0 | 1 (4.0%) |
| Nausea | 2 (5.0%) | 0 | 2 (5.0%) | 2 (8.0%) | 0 | 2 (8.0%) |
| Vomiting | 2 (5.0%) | 0 | 2 (5.0%) | 0 | 0 | 0 |
| Colitis | 4 (10%) | 0 | 4 (10%) | 0 | 0 | 0 |
| Mucositis | 0 | 0 | 0 | 2 (8.0%) | 0 | 2 (8.0%) |
| Gastritis | 2 (5.0%) | 0 | 2 (5.0%) | 0 | 0 | 0 |
| Abdominal pain | 2 (5.0%) | 0 | 2 (5.0%) | 0 | 0 | 0 |
| Appendicitis | 1 (2.5%) | 0 | 1 (2.5%) | 0 | 0 | 0 |
| Gastrointestinal, other | 3 (7.5%) | 0 | 3 (7.5%) | 0 | 0 | 0 |
| Hyperglycemia | 2 (5.0%) | 0 | 2 (5.0%) | 2 (8.0%) | 1 (4.0%) | 3 (12%) |
| Hyponatremia | 4 (10%) | 0 | 4 (10%) | 0 | 0 | 0 |
| Hypophosphatemia | 0 | 0 | 0 | 1 (4.0%) | 0 | 1 (4.0%) |
| Anorexia | 2 (5.0%) | 0 | 2 (5.0%) | 0 | 0 | 0 |
| Dehydration | 0 | 0 | 0 | 1 (4.0%) | 0 | 1 (4.0%) |
| Metabolic, other | 2 (5.0%) | 1 (2.5%) | 3 (7.5%) | 0 | 0 | 0 |
| Alk phos/ALT/AST elevated | 2 (5.0%) | 1 (2.5%) | 3 (7.5%) | 3 (12%) | 0 | 3 (12%) |
| Hyperbilirubinemia | 1 (2.5%) | 0 | 1 (2.5%) | 1 (4.0%) | 0 | 1 (4.0%) |
| Hepatic encephalopathy | 0 | 0 | 0 | 0 | 0 | 1 (4.0%) |
| Hepatitis | 0 | 0 | 0 | 1 (4.0%) | 0 | 1 (4.0%) |
| Pneumonitis | 2 (5.0%) | 0 | 3 (7.5%) | 0 | 0 | 0 |
| Dyspnea | 2 (5.0%) | 1 (2.5%) | 3 (7.5%) | 0 | 0 | 0 |
| Respiratory, other | 2 (5.0%) | 0 | 2 (5.0%) | 0 | 0 | 0 |
| Hypotension/Hypertension | 2 (5.0%) | 0 | 2 (5.0%) | 1 (4.0%) | 0 | 1 (4.0%) |
| Giant cell arteritis | 0 | 1 (2.5%) | 1 (2.5%) | 0 | 0 | 0 |
| Vascular, other | 2 (5.0%) | 0 | 2 (5.0%) | 0 | 0 | 0 |
| Encephalopathy/Memory loss | 2 (5.0%) | 0 | 2 (5.0%) | 0 | 0 | 0 |
| Muscle weakness | 0 | 0 | 0 | 1 (4.0%) | 0 | 1 (4.0%) |
| Anxiety/Confusion | 2 (5.0%) | 0 | 2 (5.0%) | 0 | 0 | 0 |
| Hypo/Hyperthyroidism | 0 | 1 (2.5%) | 1 (2.5%) | 0 | 0 | 0 |
| Thyroiditis & Hypophysitis | 1 (2.5%) | 0 | 1 (2.5%) | 0 | 0 | 0 |
| Sinus tachycardia | 1 (2.5%) | 0 | 1 (2.5%) | 0 | 0 | 0 |
| Rash, maculo-papular | 1 (2.5%) | 0 | 1 (2.5%) | 0 | 0 | 0 |
| Diplopia/Eye pain/Blurred vision | 1 (2.5%) | 0 | 1 (2.5%) | 0 | 0 | 0 |
| Weight loss | 1 (2.5%) | 0 | 1 (2.5%) | 0 | 0 | 0 |
| **Worst grade overall** | **24 (60%)** | **8 (20%)** | **33 (83%)** | **11 (44%)** | **3 (12%)** | **15 (60%)** |

# Figures

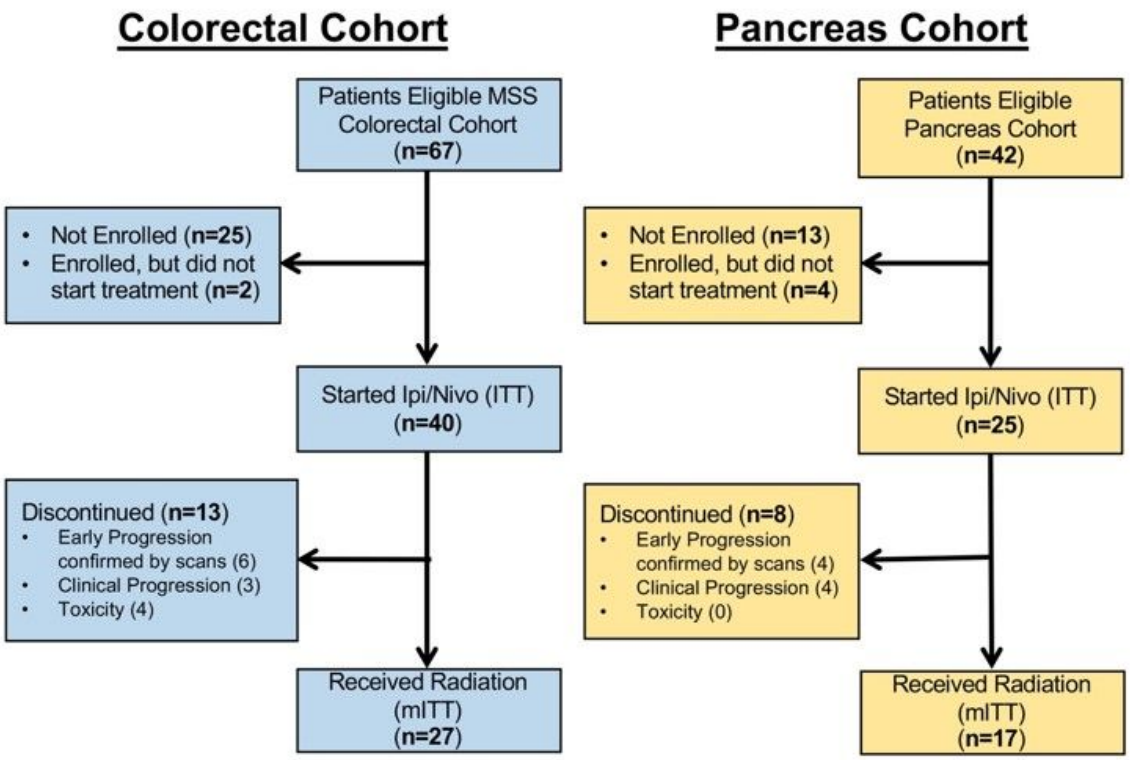


## Figure 1

Consort diagram of enrolled patients. Shown are the patients that were enrolled who started treatment (ITT) and those who received radiation (per protocol).

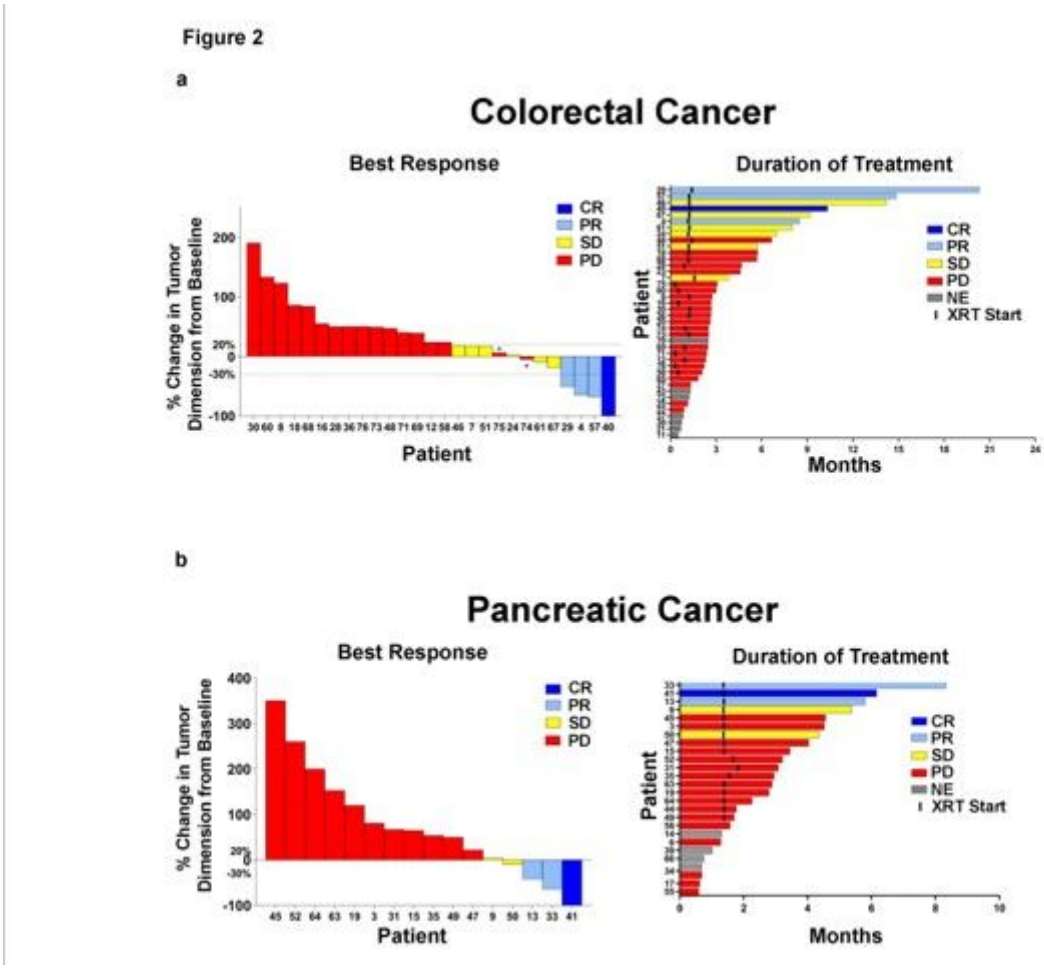


## Figure 2

Response to treatment by change in measurable disease. a, Percent (%) change in tumor dimension of comparable lesion(s) at best response for the per protocol colorectal cancer cohort and duration of treatment for the ITT colorectal cancer cohort. b, Percent (%) change in tumor dimension of comparable lesion(s) at best response for the per protocol pancreatic cancer cohort and duration of treatment for the ITT pancreatic cancer cohort. Bars color coded for responders (SD – yellow, PR/CR – blue) and non-responders (PD. – red). Non-evaluable (NE - gray) and XRT start time (black bar). Of note: patient #44 received radiation but progressed prior to scans. *unequivocal PD due to new metastatic lesions

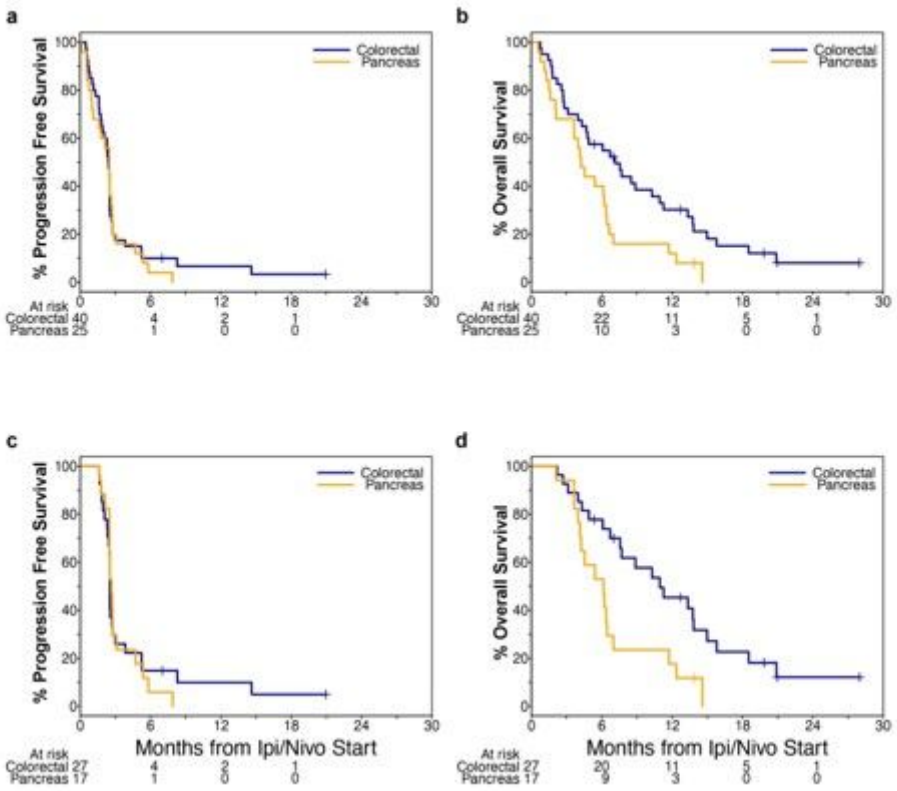


## Figure 3

Progression-free and overall survival analysis. a, b, Kaplan-Meier curve of progression-free survival (a) and overall survival (b) of patients in ITT cohort. The CRC cohort had a median PFS 2.4 months and median OS of 7.1 months. The PDAC cohort had a median PFS of 2.5 months and median OS of 4.2 months. c, d, Kaplan-Meier curve of progression-free survival (c) and overall survival (d) of patient in per protocol cohort. The CRC cohort had a median PFS of 2.5 months and median OS of 10.9 months. The PDAC cohort had a median PFS of 2.7 months and median OS of 6.1 months.

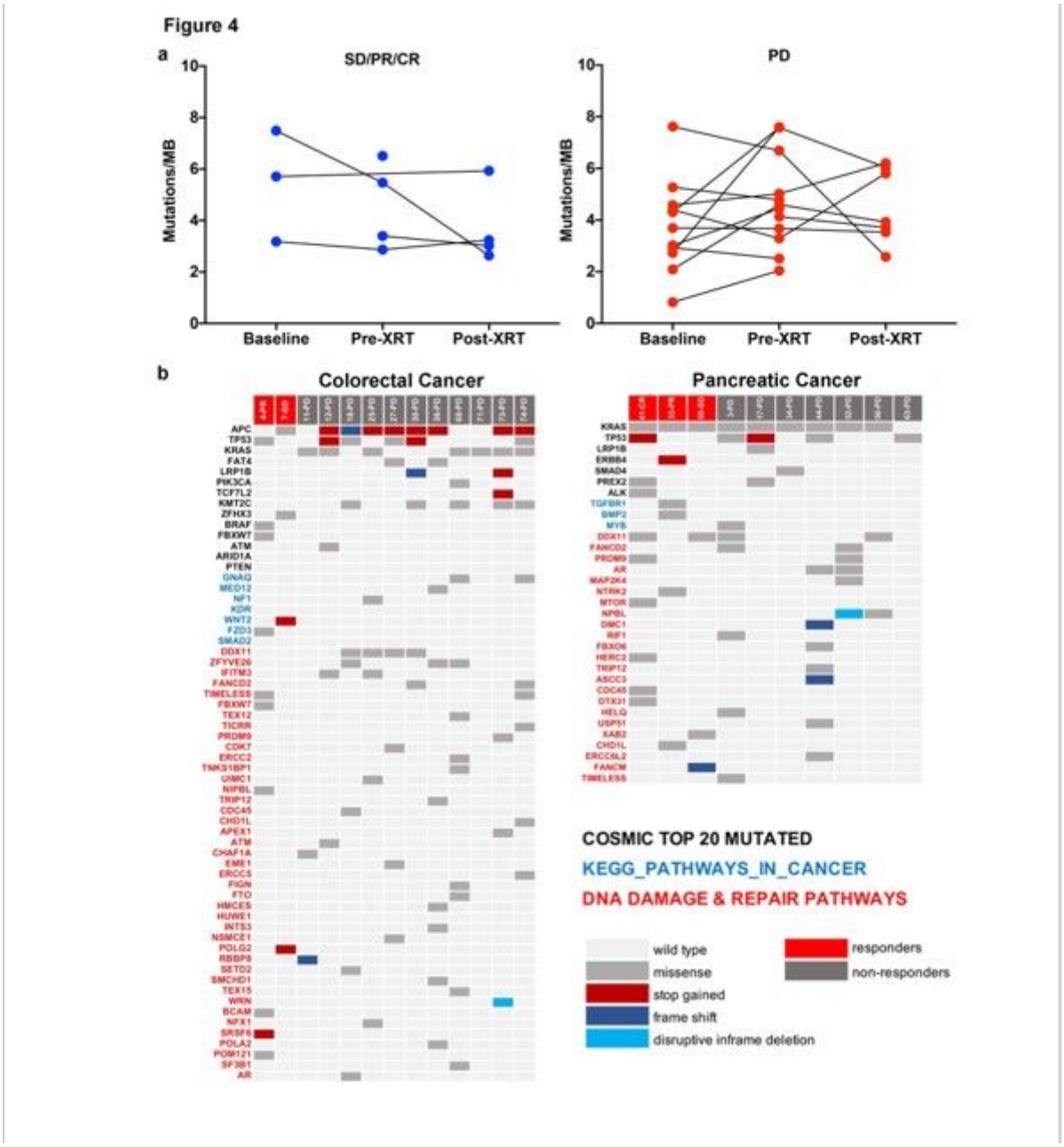


## Figure 4

Tumor mutational burden and exome mutations in patients. a, Tumor mutational burden (TMB) measured in mutations per megabase (MB) in baseline, Pre-XRT, Post-XRT biopsies. In patients with disease control (left: SD/PR/CR) and progressive disease (right: PD). b, Curated non-synonymous mutations in whole exome sequencing of colorectal and pancreatic cancer biopsies listing most commonly mutated genes from COSMIC (black), KEGG_PATHWAYS_IN_CANCER (blue), and DNA DAMAGE & REPAIR PATHWAYS (red). Mutation type color coded in legend and responders (SD/PR/CR) in red and non-responders (PD) in gray.

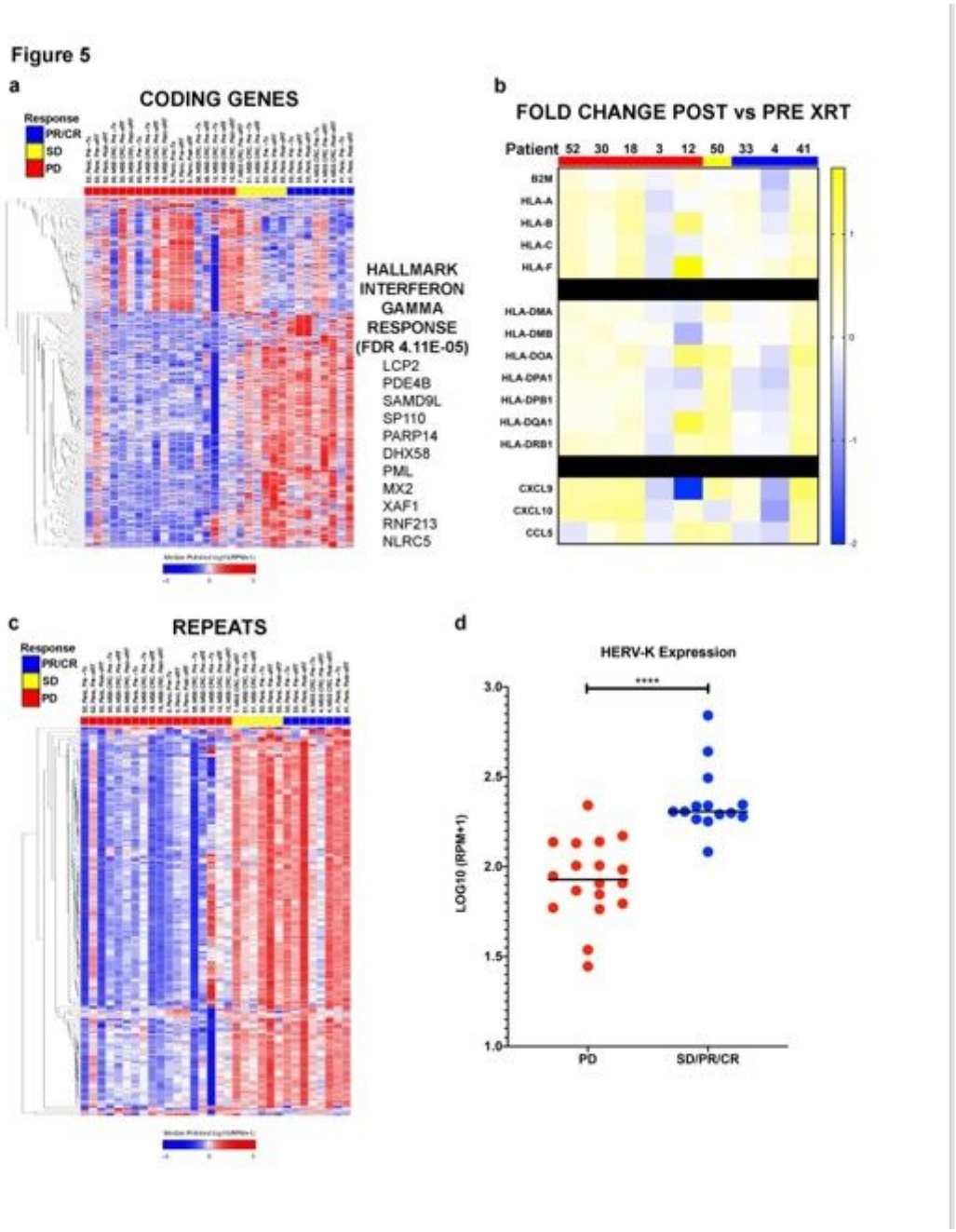


## Figure 5

Interferon response gene pathways and repeat RNA expression differences in patients. a, Unsupervised hierarchical clustering of differentially expressed coding genes (FDR < 0.05) in all biopsies from responders (SD/PR/CR – yellow/blue) compared to non-responders (PD). Interferon gamma response genes significantly enriched in genes higher in responders compared to non-responders. Significant genes shown with gene enrichment FDR for HALLMARK INTERFERON GAMMA RESPONSE. b, Fold change of major histocompatibility complex genes and cytokines that were differentially expressed genes in paired biopsies (FDR < 0.05) before and after radiation in available specimens. Scale: yellow upregulated and blue downregulated. c, Unsupervised hierarchical clustering of differentially expressed repeat RNAs (FDR < 0.05) in all biopsies from responders compared to non-responders. d, Scatter plot of HERV-K RNA

expression in LOG10(RPM+1) in non-responders (PD -red) and responders (SD/PR/CR – blue). Bar = mean. **** t-test p < 0.0001

## Supplementary Files

This is a list of supplementary files associated with this preprint. Click to download.

- SupplementaryFig1.pdf
- SupplementaryTables080420.docx